Observation and quantification of three-dimensional crack propagation in poly-granular graphite

T. J. Marrow[1,a], M. Mostafavi[1,b], S. A. McDonald[2,c] and P. M. Mummery[3,d]

[1] Department of Materials, University of Oxford, Parks Road, UK

[2] School of Materials, The University of Manchester, Manchester, UK

[3] School of Mechanical, Civil and Aerospace Engineering, The University of Manchester, Manchester, UK

[a] james.marrow@materials.ox.ac.uk [b] mahmoud.mostafavi@materials.ox.ac.uk

[c] sam.mcdonald@manchester.ac.uk [d] paul.m.mummery@manchester.ac.uk

Keywords: Nuclear graphite, computed x-ray tomography, digital volume correlation, crack propagation

Abstract. Our observations of fracture are generally restricted to the surface of test specimens; yet the fracture process occurs within the material. X-ray computed tomography (CT) can provide valuable insights into the failure process inside the material: when X-ray CT is combined with digital volume correlation (DVC) the response to applied loads of the displacement field within the material can be measured with high precision. In this paper we study the fracture behaviour of a short-bar chevron notch specimen fabricated from polygranular nuclear graphite - a quasi-brittle material. Tomographic absorption contrast images were obtained from the specimen before and after crack propagation. The DVC-measured displacement field was used to visualise the crack, and also to measure and map its opening displacement in 3D. Three-dimensional finite element simulation of the specimen obtained the relations between crack length, opening displacement and stress intensity factor along the crack front. The experimentally calculated crack opening displacements were consistent with the FE-predicted values, and could be used to obtain the critical stress intensity factor for crack propagation.

Introduction

Quasi-brittle fracture is an emergent property of inhomogeneous brittle materials: a simple network of individually brittle elements of variable strength exhibits the characteristic damage tolerant graceful failure of a quasi-brittle material; as loading progresses, failures of individual elements occur and coalesce to form cracks, while elastic strains are distributed in the remaining structure. The cracks in the network reduce its stiffness and relax the available elastic energy. The network's ultimate failure depends on the balance between the release of this stored elastic energy and the energy absorbed by fractures of individual elements. The gracefulness of this failure is affected by the distributions of strength, stiffness and the connectivity of the brittle elements. These are properties of a quasi-brittle material's microstructure, and they have a direct effect on the strength and damage tolerance of structures, so studying the interactions between microstructure, damage and mechanical behaviour in such materials is a valuable contribution to the improvement of their structural integrity assessment.

Graphite is an important component in several designs of nuclear fission reactors; for instance the structural integrity of the graphite moderators is critical to the continued safe operation of the UK's Advanced Gas Reactors (AGR). Radiolytic oxidation degrades nuclear graphite strength while, amongst other effects, fast neutron irradiation causes dimensional changes. Ultimately their combined effect may develop tensile stresses sufficient to cause damage to the reactor core. We have shown that non-irradiated nuclear graphite's fracture is preceded by the development of a

micro-cracked fracture process zone, and that this has a significant effect on its fracture resistance [1]; thus it can be classified as a quasi-brittle material.

We have previously shown that the two-dimensional digital image correlation (DIC) technique can be used to study in-situ damage nucleation and propagation [2-4]. The displacement field can readily be converted into a strain field and, if the material constitutive law is known, the stress field may also be derived. DIC is confined to studies of damage nucleation and propagation on the surface of specimens: yet damage propagates within the specimen. Measurements of the full three-dimensional displacement field within the material by the three-dimensional digital volume correlation (DVC) technique [5-7] could provide useful insights and quantitative measurements of the processes of damage development.

This paper reports a feasibility study employing X-ray computed tomography (CT) and digital volume correlation (DVC) to study crack propagation in non-irradiated virgin nuclear graphite, with measurement of crack dimensions and opening displacements in response to load. The critical stress intensity factor for stable crack propagation was also obtained via a three-dimensional finite element simulation of the short-bar chevron notch test specimen.

Methodology

Experiment: A short-bar chevron notched specimen (Fig. 1) was designed, based on the recommendations of the International Society of Rock Mechanics [8]. It was loaded by inserting a sharp steel wedge (with an angle of 10 degrees) into the notch (see Fig. 1b); this is to initiate a crack at the tip of the chevron notch that will propagate in stable equilibrium. This type of specimen allows controlled stable crack propagation in brittle or quasi-brittle materials. The experimental screw-driven loading rig ("DEBEN machine") and part of the specimen can be seen in Fig. 1c. The Perspex tube is X-ray transparent, allowing live observations by radiography in a plane perpendicular to the notch to monitor the specimen loading, followed by X-ray computed tomography scans. The experiment was carried out at the Manchester X-ray Imaging Facility (University of Manchester), using the 320 kV Nikon Metris custom bay lab instrument at a voxel size of 8 μm with a 2000 × 2000 pixel detector; 2000 radiographs were obtained over a 360° rotation for each scan and reconstructed to obtain a three-dimensional absorption tomograph with a volume of approximately 16 × 16 × 16 mm. Graphite has sufficiently low X-ray attenuation that the portions of the sample outside this region of interest did not significantly affect the reconstruction by standard back-projection algorithms (the sample diameter is 25 mm); post-processing for the influence of sample geometry was therefore unnecessary. The initial CT scan was taken with the specimen inside the Perspex tube without any load. The wedge was then driven in the specimen, to initiate and propagate a crack, at a displacement rate of 0.1 mm/min until an applied load of 250 N was attained. With the wedge in place, a second CT scan was recorded. A third scan was performed after removal of the wedge. Examples of the data are shown in Fig. 2 for the first (unloaded) and second (loaded) CT scans.

Finite Element Analysis: A finite element analysis, using ABAQUS, was carried out to simulate the specimen; an overview of the mesh, which used quadratic elements, is shown in Fig. 3a (considering symmetry, only one quarter of the specimen was modelled). The loading plane was judged to be far sufficiently from the crack tip to neglect the local effects of contact between the steel wedge and specimen; hence the steel wedge and its contact with the specimen were not simulated. As the steel wedge is rigid compared to the graphite - the Young's modulus of steel is ~200 GPa, compared to ~11 GPa for graphite [9] - the model was constrained so that nodes along the notch edge, which were all in contact with the wedge, were equally displaced to open the crack. The reaction load to the applied displacement, and hence the load applied to the wedge, was obtained. Nodes along a straight crack front were released manually, at 1 mm intervals in 22 steps

from *a/W*=0.043 to 0.96, to simulate different crack lengths (see Fig. 3b). The elastic strain energy release rate (*J*-integral) with crack propagation was calculated within ABAQUS by the contour integral method [10], from which the mode I plane strain stress intensity factor was obtained. Collapsed nodes, or singular elements, were not used since they do not affect the energy release rate calculated [11] by contour integral methods [12]. The elastic properties for typical near-isotropic nuclear graphite were assumed: Young's modulus, 10.9 GPa, and Poisson's ratio, 0.2 [9].

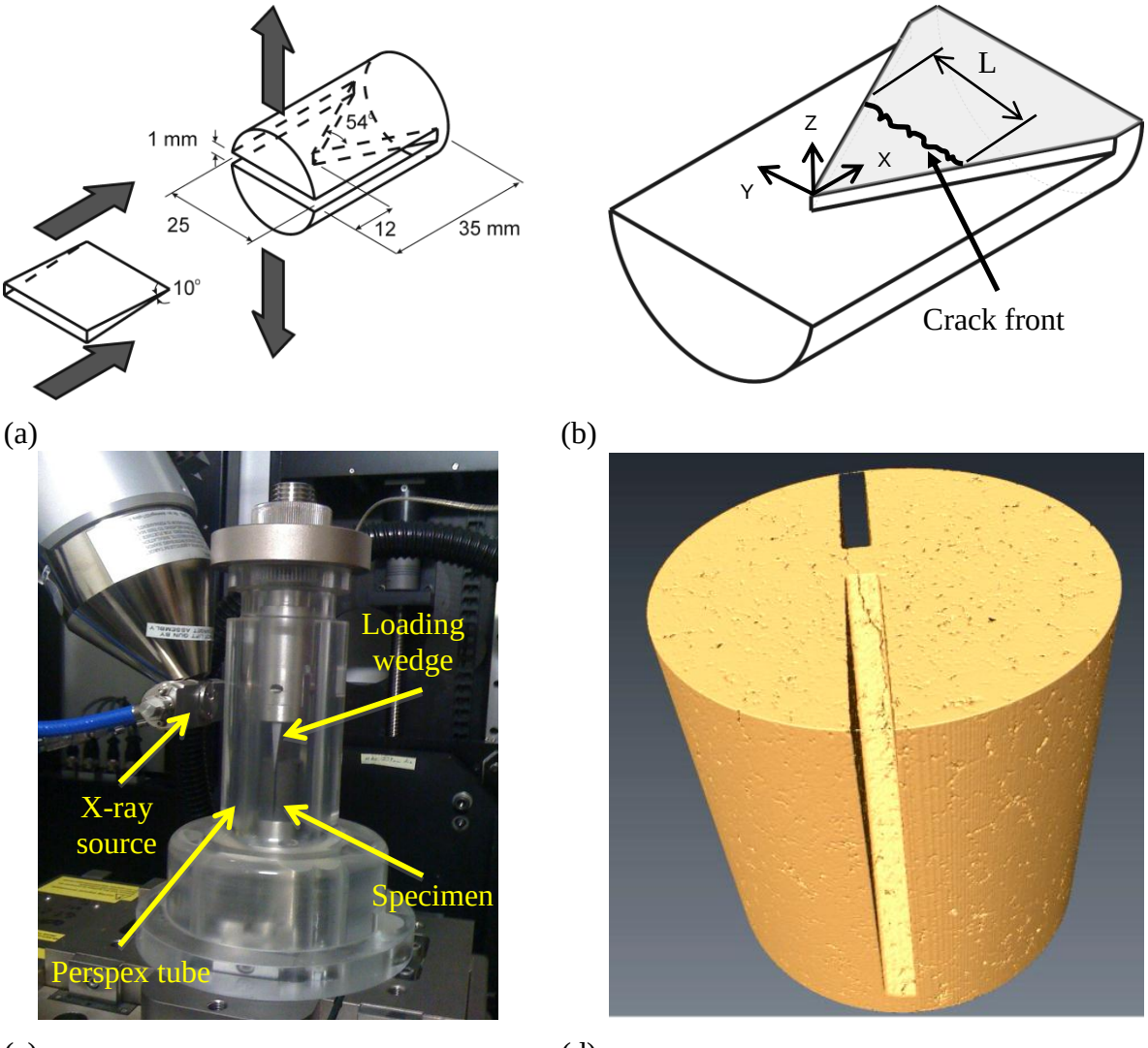

(a) (b)

(c) (d)

Fig. 1. Overview of the short-bar chevron notch specimen (a) dimensions of the specimen (b) half the specimen - the crack initiates from the notch tip and propagates toward the end the specimen (c) specimen within the loading rig (d) reconstructed tomography scan of the investigated region of the specimen after loading.

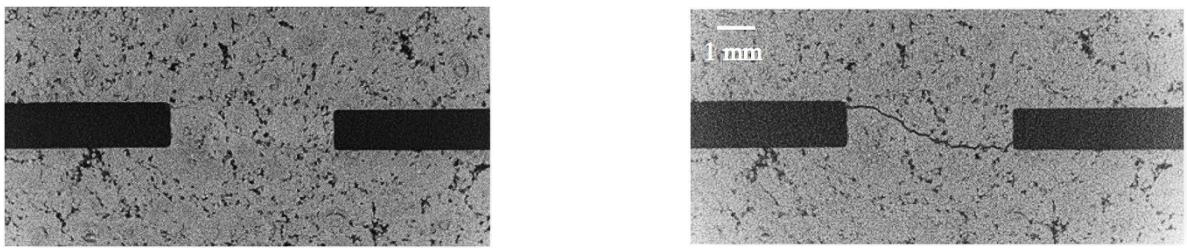

(a) (b)

Fig. 2. CT data (sections in the YX plane, 3 mm below the notch tip); (a) unloaded and (b) loaded.

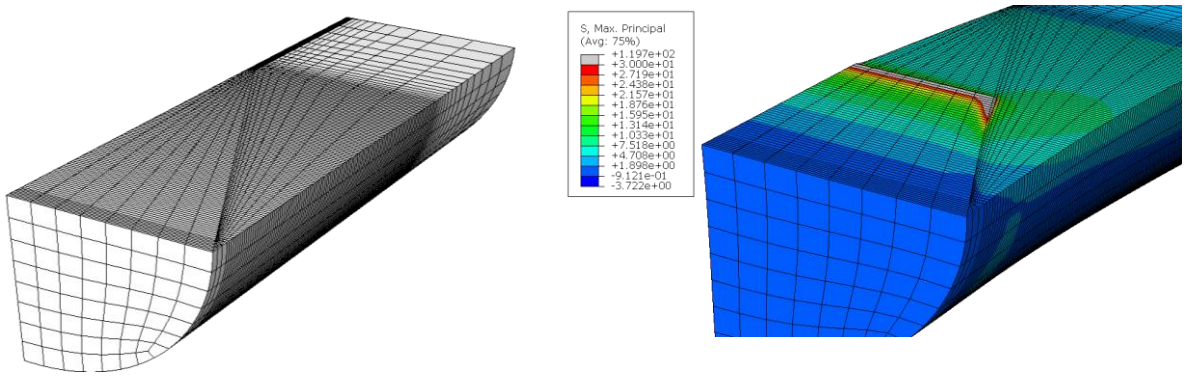

(a) (b)

Fig. 3. Finite element simulation; (a) Mesh (b) Maximum principal stress

Results

Finite element: As quadratic elements were used, two sets of FE outputs may be obtained: one for the values obtained at the element corner nodes and the other at the mid-side-nodes. It has been shown that using the corner nodes gives a better representation of energy release rate [13], thus data from these nodes were selected. The obtained mode I stress intensity factor varied along the crack front, with a minimum at the surface to a maximum at the centre. The variation decreased with increasing a/W: from K_{max}/K_{min} = 1.66 for a/W = 0.043 to 1.12 for a/W = 0.65; there was less than 10% difference for a/W>0.65. An example for a/W=0.23 is shown in Fig. 4, as the variation of normalised stress intensity factor, K_N, along the crack front:

$$K_N = \frac{K}{s\sqrt{a}}$$

where σ is the nominal opening stress (σ = F/A; F is the applied force and A is the area of the ligament ahead of the crack front).

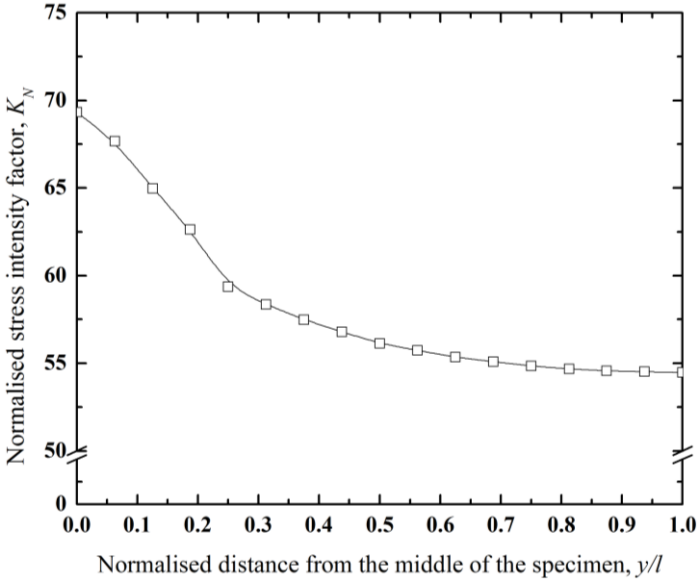

Fig. 4. Variation of normalised stress intensity factor as a function of the normalised distance along the crack front at a/W = 0.23 (the full width of the crack front is 2l).

Digital volume correlation: The CT datasets were correlated using a window size of 256×256×256 voxels followed by 32×32×32 voxels with 50% overlap. To estimate the accuracy of the digital volume correlation analysis, the strain noise (standard deviation in maximum normal strain) in a region remote from (i.e. 7 mm ahead of) the crack tip was measured. The predicted compressive strain in the same region is 4.2×10^{-5}. The strain noise, obtained by correlation between the first and third unloaded scans in a region well away from the crack, between which there was only rigid body movements, was 3.2×10^{-4}, corresponding to a displacement measurement uncertainty of 1.5 µm.

Fig. 5a and b shows an example of the displacement data, and visualisation of the crack opening using the maximum normal strain obtained from the displacement gradients. A 3D visualisation of the crack is shown in Fig. 5c; the red colour denote high levels of opening displacement (i.e. high strain) and blue colour, lower levels. It should be noted that the strains due to crack opening are nominal.

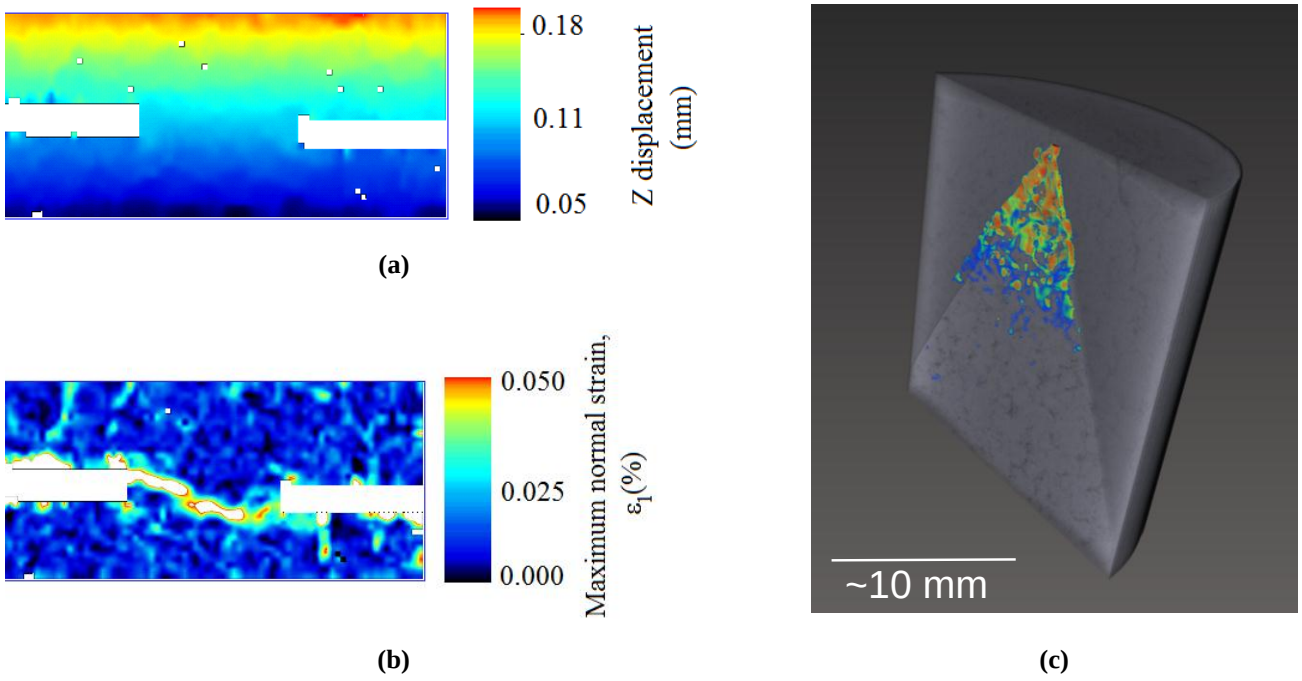

Fig. 5. Visualisation of the crack following DVC analysis (a) contour of z displacement (i.e. perpendicular to notch plane) in the y-z plane at x = 3 mm from the tip of the notch (b) contour of maximum normal strain at x = 3 mm from the tip of the notch (c) 3D visualisation of the crack using the maximum normal strain.

The DVC data allow the crack opening displacement under load to be measured. Its variation across the crack surface was mapped: to do this efficiently for the large number of measurements, at each point, the displacement vectors along a line orthogonal to the notch plane were extracted; a fifth-order polynomial was fitted to the displacements along the line and the difference between its maximum and minimum was taken as an estimate of the crack opening displacement (COD). The data are shown in Fig. 6, which shows the crack opening is greatest close to the notch tip, as to be expected, and that the crack front is uneven. The average crack length obtained in this way is 5.2 mm. Using the CT images alone, and relying on contrast to estimate the crack tip, the observed crack length at the specimen centre is 4.3 mm, compared to 5.4 mm at the same position by COD measurement using DVC with a threshold of 0.007 mm. (Values below 0.007 mm, based on the average values obtained by this procedure at positions remote from the crack tip are regarded as below the noise level and are treated as zero).

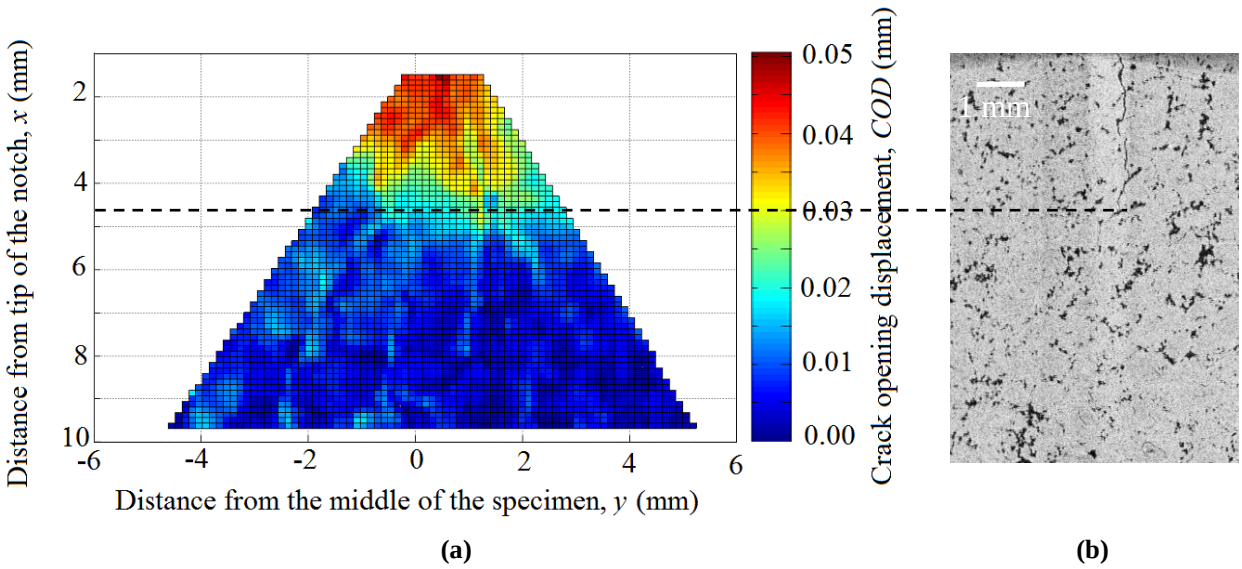

Fig. 6. Crack opening displacements and crack length measurement: a) map of the net crack opening displacement (mm) under load, the observed crack length at the centre is 5.4 mm; b) CT data only at the specimen centre. The horizontal line marks the position of the crack tip (4.3 mm) observed in the CT image at the specimen centre.

Discussion

Digital volume correlation analysis of X-ray computed tomography data has been employed to study the 3D opening of a crack, propagated in a short-bar chevron notch specimen. The crack can be visualized (Fig. 5) as an area of high artificial strain, which is due to crack opening displacement. Comparison of crack length measurement by visual observation of the crack (in the CT data) and the crack opening displacement data (Fig. 6) shows that DVC is more sensitive than X-ray CT in locating the crack front.

The map of crack opening displacements (Fig. 6) shows that the crack tends to open more in the centre of the specimen, compared to the edges. This is consistent with the greater mode I stress intensity factor that is predicted towards the specimen centre (Fig. 4). The data also show that the crack tends to open more towards one edge than the other; this might be attributed to a misalignment of the loading wedge, and further demonstrates the sensitivity of DVC measurements. The uneven crack front is attributed to local interactions with the coarse nuclear graphite microstructure, which contains particles up to 1 mm in size from the Gilsonite coke particles [9]

The measured opening displacements may be compared with the FE simulation. To do this, the average crack opening displacement across the crack, as a function of distance from the notch tip, was obtained. The data shown in Fig. 7, together with the opening profile predicted by the finite element simulation for a crack with 5.2 mm length, which was the measured average. A good fit is obtained between the profiles when the stress intensity factor, K, is 1.61 MPa.m$^{1/2}$ (1.55 to 1.72 MPa.m$^{1/2}$ with 95% confidence). This value is comparable to values obtained in different specimen geometries of the same material [1, 14]. The differences can be attributed to the inelastic behaviour of graphite in front of the crack tip which forms a fracture process zone, the size of which depends on specimen geometry [15].

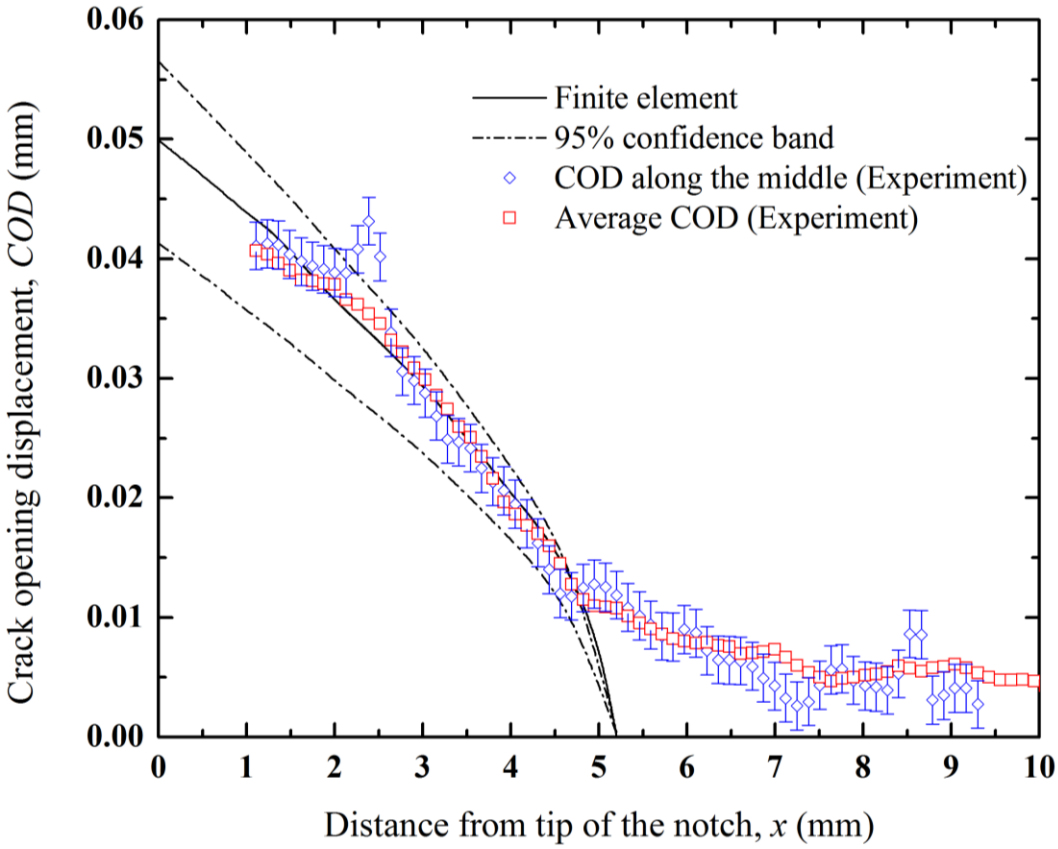

Fig. 7. Comparison between crack opening profiles of average measured (DVC) data and finite element simulated. Average crack length is 5.2 mm and K=1.61 MPa. m$^{1/2}$ (1.55 to 1.72 MPa.m$^{1/2}$ with 95% confidence)

Fig. 6 therefore shows that a continuous macromechanical crack front that separates the cracked and uncracked regions cannot be defined, consistent with experimental observations of the development of a microcracked fracture process zone ahead of the fully open crack front [2]. It may be argued that a theoretical, asymptotic stress, strain or displacement distribution cannot be accurately fitted to the experimental measurements to characterise the mechanical driving force for crack propagation, since the tip of the crack cannot be defined with confidence. The stress intensity factor obtained here by fitting to the crack opening profile is an approximation. It is suggested that direct calculation of energy release rate, which is the thermo-dynamic mechanical driving force for crack propagation, requires a method that is not dependent on an accurate location of the crack tip. A method to do this has been developed by the authors to calculate the elastic strain energy release rate from direct digital image correlation observations in 2D, based on the contour integral method [16]; this is now being developed for 3D application.

Acknowledgements

Authors would like to thank the Manchester X-ray Imaging Facility for the award of beam time. Ms. Aurore Fargette is thanked for her assistance with the tomography experiment. TJM and MM acknowledge the support of the Oxford Martin School and EDF Energy (GRA/GNSR/6041). Dr Richard Boardman and Professor Ian Sinclair, μVis centre, University of Southampton, are gratefully acknowledged for their assistance with 3D visualization of the strain data. The opinions expressed are those of the authors.

References

1. Mostafavi, M. and T.J. Marrow, *Quantitative in situ study of short crack propagation in polygranular graphite by digital image correlation.* Fatigue and Fracture of Engineering Materials and Structures, 2012. **In Press**.
2. Mostafavi, M. and T.J. Marrow, *In situ observation of crack nuclei in poly-granular graphite under ring-on-ring equi-biaxial and flexural loading.* Engineering Fracture Mechanics, 2011. **78**(8): p. 1756-1770.
3. Cook, A., J. Duff, N. Stevens, S. Lyon, A.H. Sherry, and T.J. Marrow, *Preliminary evaluation of digital image correlation for in-situ observation of low temperature atmospheric-induced chloride stress corrosion cracking in austenitic stainless steels.* ECS Transactions, 2010. **25**(37): p. 119-132.
4. Marrow, T.J., D. Gonzalez, M. Aswad, J.Q. Da Fonseca, and P.J. Withers, *In-situ observation and modelling of intergranular cracking in polycrystalline alumina.* Key Engineering Materials, 2011. **465**: p. 507-510.
5. Bay, B.K., T.S. Smith, D.P. Fyhire, and M. Saad, *Digital volume correlation: three-dimensional strain mapping using X-ray tomography.* Experimental Mechanics, 1999. **39**(3): p. 217-226.
6. Franck, C., S. Hong, S.A. Maskarinec, D.A. Tirrell, and G. Ravichandran, *Three-dimensional full-field measurements of large deformations in soft materials using confocal microscopy and digital volume correlation.* Experimental Mechanics, 2007. **47**: p. 427-438.
7. Smith, T.S., B.K. Bay, and M.M. Rashid, *Digital volume correlation including rotational degrees of freedom during minimization.* Experimental Mechanics, 2004. **42**(3): p. 272-278.
8. Ouchterlony, F., *International society for rock mechanics commission on testing methods - Suggested methods for determining the fracture toughness of rock.* International Journal of Rock Mechanics and Mining Sceinces, 1988. **25**(2): p. 71-96.
9. Joyce, M.R., T.J. Marrow, P.M. Mummery, and B.J. Marsden, *Observation of microstructure deformation and damage in nuclear graphite.* Engineering Fracture Mechanics, 2008. **75**(2): p. 3633-3645.
10. ABAQUS, *User's Manual*2009: ABAQUS Inc., Providence, Rhode Island, Version 6.9.
11. Sinclair, G.B., *Some inherently unreliable practices in present day fracture mechanics.* International Journal of Fracture, 1985. **28**: p. 3-16.
12. Li, F.Z., C.F. Shih, and A. Needleman, *A comparison of methods for calculating energy release rates.* Engineering Fracture Mechanics, 1985. **21**(2): p. 405-421.
13. Brocks, W. and I. Scheider, *Numerical aspects of the path-dependece of the J-integral in incremental plasticity - How to calculate reliable J-values in FE analyses*, 2001, Institute für Werkstofforschung: Köln-Porz.
14. Marrow, T.J., A.D. Hodgkins, M.R. Joyce, and B.J. Marsden, *Damage nucleation in nuclear graphite.* Energy Materials, 2006. **1**(3): p. 167-170.
15. Becker, T.H., T.J. Marrow, and R.B. Tait, *Damage, crack growth and fracture characteristics of nuclear grade graphite using the Double Torsion technique.* Journal of Nuclear Materials, 2011. **414**(1): p. 32-43.
16. Becker, T.H., M. Mostafavi, R.B. Tait, and T.J. Marrow, *An Approach to Calculate the J-Integral by Digital Image Correlation Displacement Field Measurement* Fatigue and Fracture of Engineering Materials and Structures, 2012. **In press**.